



## Subseafloor stratigraphic profiling and soil classification from piezocone tests: A case study in the Gulf of Lion (NW Mediterranean Sea)

**S. Lafuerza, J. Frigola, and M. Canals**

*GRC Geociències Marines, Departament d'Estratigrafia, Paleontologia i Geociències Marines, Universitat de Barcelona, Martí i Franquès s/n, E-08028 Barcelona, Spain (miquelcanals@ub.edu)*

**G. Jouet**

*Institut Français de Recherche pour l'Exploitation de la Mer, BP 70, F-29280 Plouzané, France*

**M. Bassetti**

*IMAGES, Université de Perpignan Via Domitia, 52 avenue Paul Alduy, F-66860 Perpignan, France*

**N. Sultan**

*Institut Français de Recherche pour l'Exploitation de la Mer, BP 70, F-29280 Plouzané, France*

**S. Berné**

*IMAGES, Université de Perpignan Via Domitia, 52 avenue Paul Alduy, F-66860 Perpignan, France*

[1] We show the results provided by piezocone tests in determining the stratigraphic profile and the soil classification of two drilling sites in the outer shelf and the upper slope of the Gulf of Lion, PRGL2 and PRGL1, respectively. Correlations with grain-size data indicate that sleeve friction can be used for profiling fine-grained sediments (site PRGL1), whereas cone tip resistance is the most adequate for sequences made of alternations of coarse- and fine-grained intervals (site PRGL2). Normalized cone resistance and friction ratio proved to be also appropriate for soil stratigraphy as it depicts trends in the coarse fraction of the tested soil. Silts and clays present in similar proportions at site PRGL1 responded to piezocone testing as pure clays usually do. Consequently, classical soil classification methods resulted in erroneous interpretation of these sediments as clays, whereas classification of the heterogeneous deposits at PRGL2 was consistent with the grain size. When tied to a high-resolution seismic reflection profile, the stratigraphy interpreted from the piezocone profile matches with the main seismic sequences and discontinuities defined from seismic stratigraphy analysis. Graded bedding also matches with cone tip resistance and sleeve friction data.

**Components:** 4236 words, 10 figures.

**Keywords:** piezocone; stratigraphy; soil classification; Gulf of Lion.

**Index Terms:** 3002 Marine Geology and Geophysics: Continental shelf and slope processes (4219).

**Received** 5 October 2007; **Revised** 21 March 2008; **Accepted** 22 October 2008; **Published** 30 December 2008.

Lafuerza, S., J. Frigola, M. Canals, G. Jouet, M. Bassetti, N. Sultan, and S. Berné (2008), Subseafloor stratigraphic profiling and soil classification from piezocone tests: A case study in the Gulf of Lion (NW Mediterranean Sea), *Geochem. Geophys. Geosyst.*, 9, Q12028, doi:10.1029/2007GC001845.

## 1. Introduction

[2] The EC funded “Profiles Across Mediterranean Sedimentary Systems 1” (PROMESS 1) research project was designed to obtain very long sediment cores and perform in situ physical measurements from two continental margins in the Mediterranean Sea [Berné *et al.*, 2004a]. In the Gulf of Lion, drilling and in situ testing were carried out at two sites: PRGL1 in the upper slope at 298 m of water depth (mwd) and PRGL2 in the outer shelf at 103 mwd (Figure 1). Five boreholes were drilled at site PRGL1 (PRGL1\_1 to PRGL1\_5) and two at site PRGL2 (PRGL2\_1 and PRGL2\_2). In this technical brief we compare the stratigraphic profile and soil type classification interpreted from piezocone measurements performed at sites PRGL1\_3 and PRGL2\_1 with grain size data acquired from sediment cores at PRGL1\_4 and PRGL2\_2 and with high-resolution seismic reflection profiles. The aim of this study is to illustrate the advantages of piezocone tests for (1) soil classification and stratigraphic profiling of marine sediments before drilling and (2) for the lithostratigraphic interpretation of seismic reflection profiles.

## 2. Materials and Methods

[3] Piezocone tests (CPTU) were performed using a downhole cone penetration system that enable CPTU from the base of the borehole in sites PRGL1\_3 and PRGL2\_1, reaching penetration depths of 150 and 100 mbsf, respectively. The downhole system latches into the lower end of a drill pipe by applying mud pressure in the borehole, while downhole data are recorded. The system requires a drilling apparatus for advancing the borehole and a bottom hole assembly that permits latching the thrust machine, of 90 kN capacity. The maximum stroke of the thrust machine is 3 m. This system enables the borehole to be advanced and CPTUs be performed at every depth. Direct measurements of cone tip resistance ( $q_c$ ), sleeve friction ( $f_s$ ), and pore pressure ( $u_2$ ) were recorded at a constant penetration rate of  $2 \text{ cm s}^{-1}$ . CPTU were performed before drilling for coring providing a reliable lithostratigraphic profile.

[4] Derived parameters from CPTU, such as the normalized cone resistance ( $Q_t$ ), the friction ratio (FR), and the pore pressure ratio ( $B_q$ ) (see notation section), allow the identification of the soil type using the soil classification charts proposed by Robertson [1990] and Ramsey [2002]. Both meth-

ods define nine soil classes according to  $Q_t$ /FR and  $Q_t/B_q$  ratios but numbers are referred to soil classes distinctly (Figures 2 and 3). Changes in profiles of  $q_c$ ,  $f_s$ , have been followed for delineating the stratigraphic profile and the ratio of  $Q_t$ /FR for correlating with grain size curves. The variables  $q_c$  and  $Q_t$  respond to variations in the resistance generated by the coarse fraction, whereas  $f_s$  and FR illustrate changes in the cohesive fraction, which usually corresponds to the fine-grained fraction [Lunne *et al.*, 1997].

[5] The total sediment core recovery from PRGL1\_4 and PRGL2\_2 was 300 and 100 m, respectively. Grain-size analyses were carried out in both the bulk and the carbonate free fractions using a Laser Particle Sizer (LPS) Coulter LS100 at PRGL1\_4 (J. Frigola *et al.*, personal communication, 2008) and a LSP Coulter LS230 at PRGL2\_2 [Bassetti *et al.*, 2008]. Since laser diffraction methods are claimed to underestimate plate-shaped clay mineral percentages, we consider the clay-silt limit at  $8 \mu\text{m}$  following the method proposed by Konert and Vandenberghe [1997]. The particle sizes considered are (1) clays with diameter ( $\phi$ ) between 0 and  $8 \mu\text{m}$ , (2) silts with  $8 < \phi < 63 \mu\text{m}$ , and (3) sands with  $\phi > 63 \mu\text{m}$ .

[6] Geotechnical stratigraphy derived from CPTU was correlated with the seismic stratigraphy established by several authors. Six seismic sequences (S0 to S5), corresponding to 100 ka glacial-interglacial cycles, are bounded by major erosion surfaces (D30 to D70) [Berné *et al.*, 2004a; Rabineau *et al.*, 1998, 2005; S. Berné *et al.*, Sedimentary sequences and sea-level changes during the last 500 kyrs: The Gulf of Lions revisited by the Promess 1 drilling operation, submitted to *Geochemistry, Geophysics, Geosystems*, 2008]. Within the last sequence (S5), other relevant secondary unconformities (D65, D64, D63 and D61) are identified (Jouet *et al.* [2006] and see review by Bassetti *et al.* [2008]).

## 3. Results

### 3.1. CPTU Tests at PRGL1 Site

[7] At PRGL1\_3 the cone tip resistance,  $q_c$ , and the pore water pressure,  $u_2$ , increase quasi-linearly with depth, whereas the sleeve friction,  $f_s$ , depicts a more variable profile (Figure 4). Note that the 3-m-spaced negative peaks in  $u_2$  curves are losses in CPTU readings and therefore are unrelated to soil type changes. Five geotechnical-stratigraphic units were identified based on  $f_s$  values trend. These

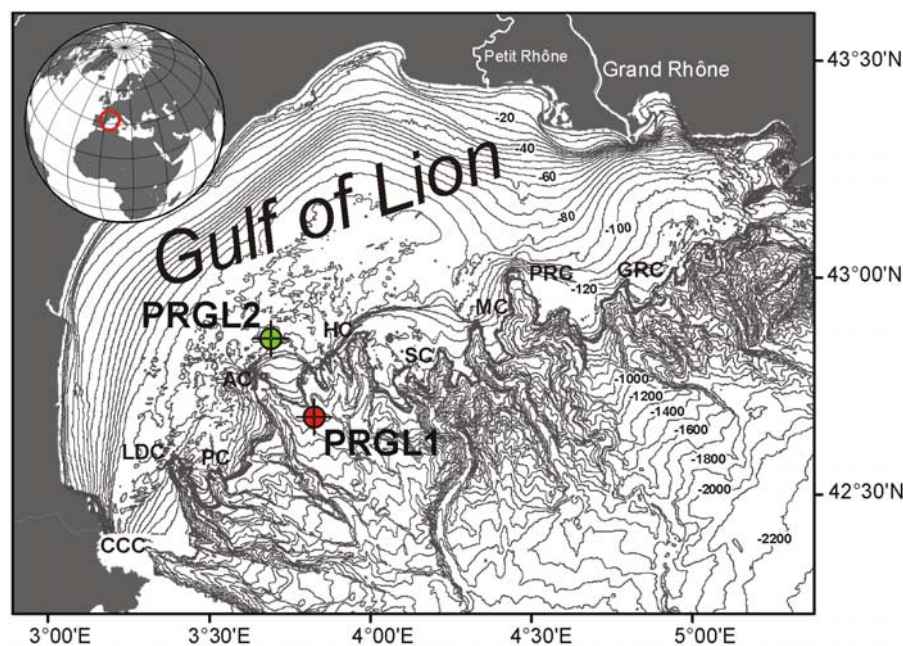


**Figure 1.** Location of the PRGL2 (42°50′58.20″N, 003°39′3085″E) and PRGL1 (42°41′23.30″N, 003°50′15.50″E) sites. CCC, Cap de Creus Canyon; LDC, Lacaze-Duthiers Canyon; PC, Pruvot Canyon; AC, Aude Canyon; HC, Hérault Canyon; SC, Sète Canyon; MC, Montpellier Canyon; PRC, Petit Rhône Canyon; GRC, Grand Rhône Canyon. Bathymetry in meters from *Berné et al.* [2004b] and *Medimap Group* [2005]. The 100 m contour equidistance unless otherwise indicated. Names after *Canals* [1985].

units have been numbered from I to V from top to bottom. Subunits are identified by alphabetical subindexes (Figure 4). Soil classifications charts in Figures 2 and 3 predict that the geotechnical unit I consists of silty clays and clays, whereas units from II to V are uniformly made by clays. Figure 4 shows the soil type based on the  $Q_t/FR$  chart from Robertson's (Figure 2) at corresponding depths.

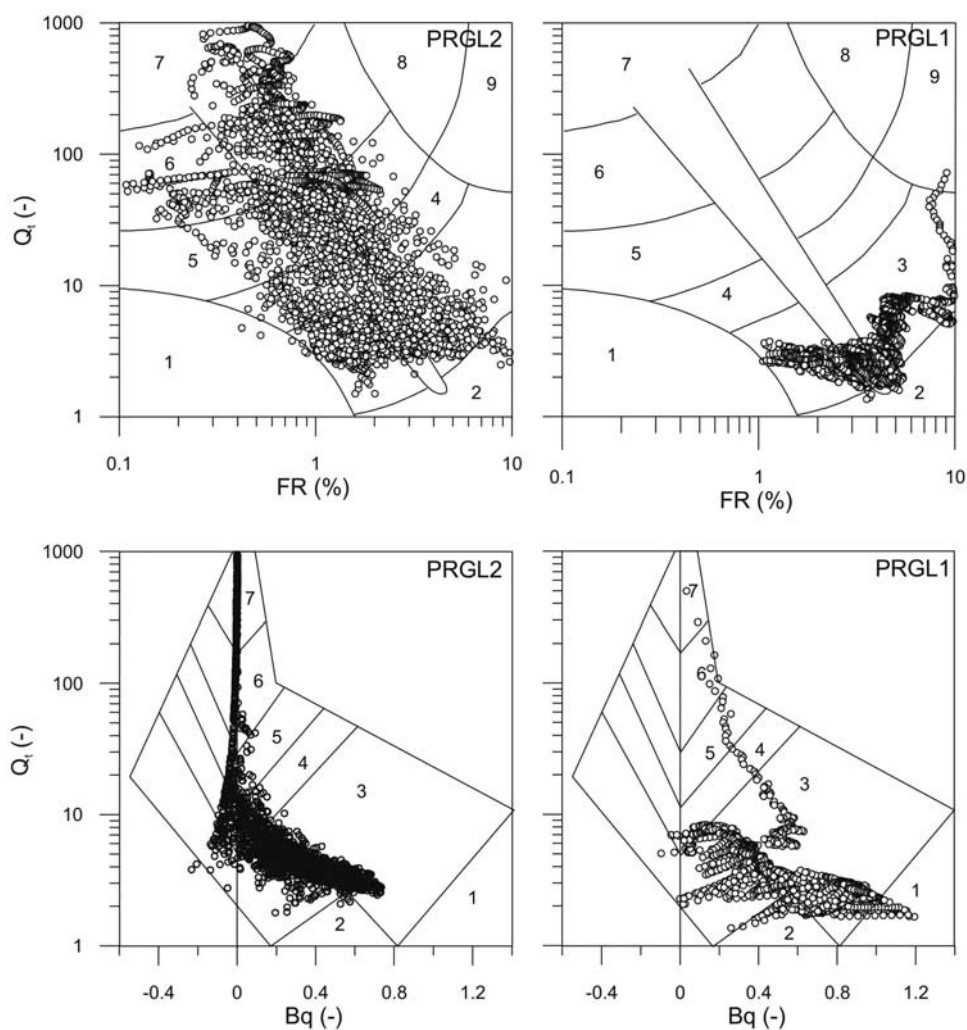
[8] Correlation of  $Q_t/FR$  and grain-size profiles illustrates the correspondence between  $Q_t/FR$  and the silt/clay ratio (Figure 5), supporting the sedimentological interpretation of the soil classes in Figures 2 and 3. Furthermore, unit boundaries (red dotted lines, Figures 4 and 5) correspond to marked decreases in clay content accompanied by an evident increase in sand fraction, as observed by increases in  $Q_t/FR$ . The coincidence of these sharp changes with the end of CPTU sequences suggests those unit boundaries at 36 and 72 mbsf can be located within units IIb and IIId, respectively. In these levels and to a lesser extent at IVd, pronounced positive peaks in  $Q_t/FR$  correspond to sand content augmentations (Figure 5). Main changes in the clay fraction, such as those in subunits IIb, IIId, and IVd are clearly identified from the  $f_s$  profile (Figure 6). The inverse variation between  $Q_t/FR$  and the clay fraction supports the

clay dependence of FR and  $f_s$ , as well as the silt dependence of  $Q_t$ . This, in addition, confirms the 8  $\mu$ m size as an adequate clay-silt limit for laser grain-size measurements.

### 3.2. CPTU Tests at PRGL2 Site

[9] In PRGL2, five geotechnical-stratigraphic units are identified based on changes in  $q_c$  (Figure 7) and named 1 to 5 from top to bottom, and subdivided using alphabetically ordered subindexes.  $q_c$  and  $f_s$  curves are highly similar, with relative high values for sands (from 0 to 28.6 mbsf and from 67 to the borehole bottom) and relative low values in clays (from 28.6 to 68 mbsf and from 78.3 to 82.3 mbsf) (Figure 8). Zero  $u_2$  values through the upper 30 m and negative values at the borehole bottom are attributed to readings in sands affected by cavitation processes [Lunne et al., 1997]. Soil types based on the  $Q_t/FR$  chart from Robertson classification at corresponding depths are also shown in Figure 7. The good correlation between the sand content profile and  $Q_t/FR$  profile supports geotechnical stratigraphy for site PRGL2. Geotechnical units have been correlated with the lithological units defined for this site by *Bassetti et al.* [2008] and we found good correlation. However, we grouped them in five major units for ease of





**Soil types from Robertson (1990):**

1 - Sensitive fine grained; 2 - Organic soils-peats; 3 - Clays; 4 - Silt mixtures clayey silt to silty clay; 5 - Sand mixtures, silty sand to sand silty; 6 - Sands; clean sands to silty sands; 7 - Gravelly sand to sand; 8 - Very stiff sand to clayey sand; 9 - Very stiff fine grained.

**Figure 2.** Soil type classifications for PRGL1 and PRGL2 sites plotted on *Robertson's* [1990] charts for normalized parameters  $Q_t$ , FR, and  $B_q$ .

consistency with resistance values, whereas the lithological profile identified 14 units [Bassetti *et al.*, 2008]. At the borehole bottom (99.24–100.13 mbsf), these authors identify a very coarse clastic unit that we have included in geotechnical subunit 5c.

[10] The soil types interpreted from CPTU classifications (Figures 2 and 3) are highly consistent with the grain size distribution (Figure 8). Graded bedding is identified from  $q_c$  at intervals where the sampling resolution from grain size analysis is insufficient to detect them. This is illustrated by the overall coarsening upward trend of subunit 1d

and the interval comprised by subunits 5b and 5c, and the fining upward trend of subunits 4a, 4b, and 4c and by subunit 5a. Changes of the fine fraction content, which is made of clayey silts, are well depicted by the  $1/Q_t$  profile.

## 4. Discussion

### 4.1. Soil Classification From CPTU Measurements

[11] Correlations of grain-size curves with CPTU sediment type classifications at site PRGL1 indi-

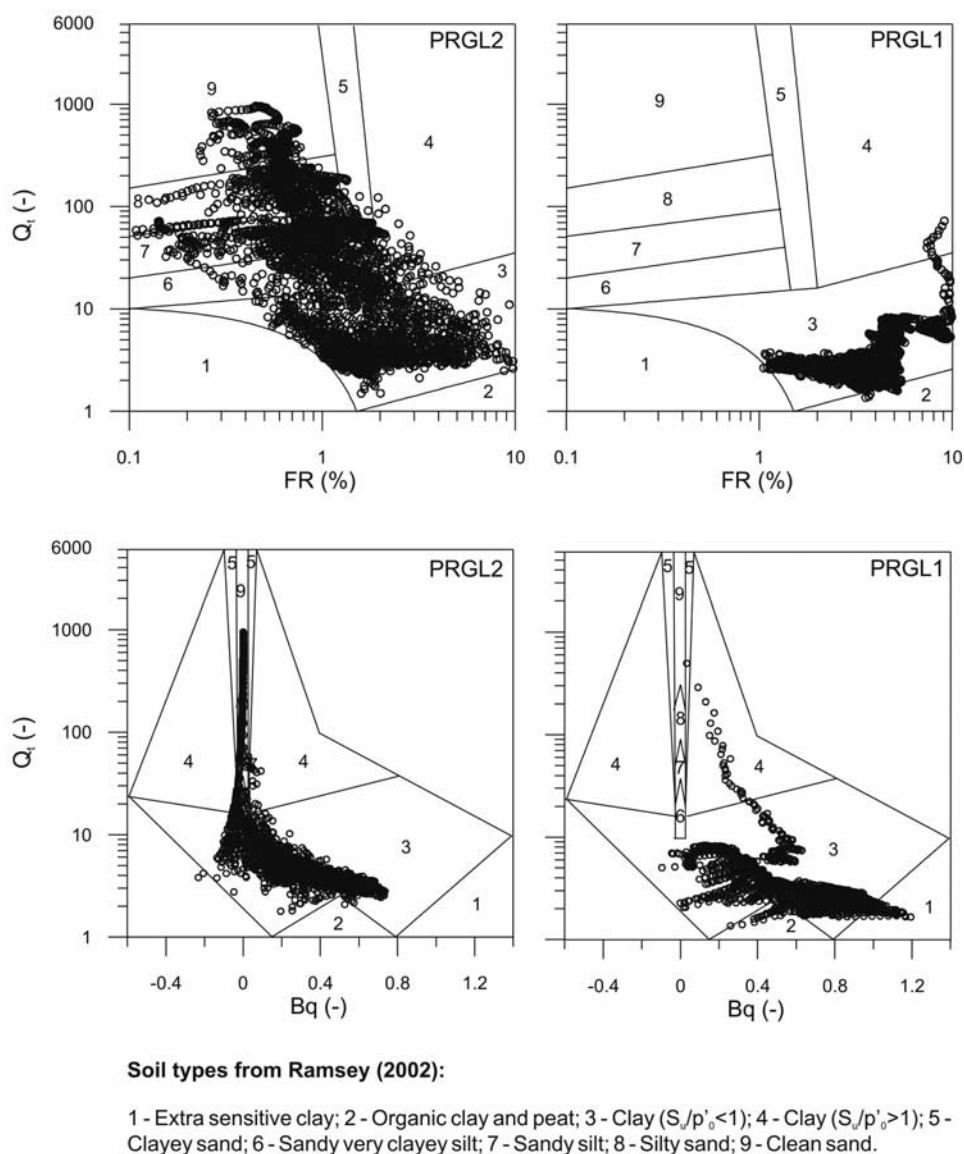


**Figure 3.** Soil type classifications for PRGL1 and PRGL2 sites plotted on Ramsey's [2002] charts for normalized parameters  $Q_t$ , FR, and  $B_q$ .

cate that the percentage of silts and clays ranges between 40 and 60% along the borehole (Figure 4). Units II to V are made of a mixture of silts and clays instead of mainly clays, as suggested by CPTU classifications (Figures 2 and 3). This can be attributed to similar (undrained) piezocone penetration of silts and clays when they occur in similar proportions. In contrast, piezocone testing in sediments with heterogeneous grain size, where drainage conditions occur [Lunne *et al.*, 1997], as in PRGL2, allows accurate sediment type attribution (Figure 7). On the other hand, in deposits where mixtures of cohesionless (silty sands to gravels) sediments are present, as in PRGL2, soil

changes are better detected from cone tip resistance,  $q_c$ , as it responds more precisely to changes in drainage conditions than sleeve friction,  $f_s$  (Figure 7).

[12] We have found a good correlation between Robertson's [1990] and Ramsey's [2002] soil classification methods. However, when cavitation occurs, as in PRGL2, the  $Q_t/FR$  ratio should be used in isolation for soil-type interpretation. Gravelly sands and sands may induce temporary cavitation adjacent to the pore water pressure sensor location, making the  $Q_t/B_q$  model unreliable [Ramsey, 2002]. For correlating with grain size we, therefore, have used only Robertson's [1990]

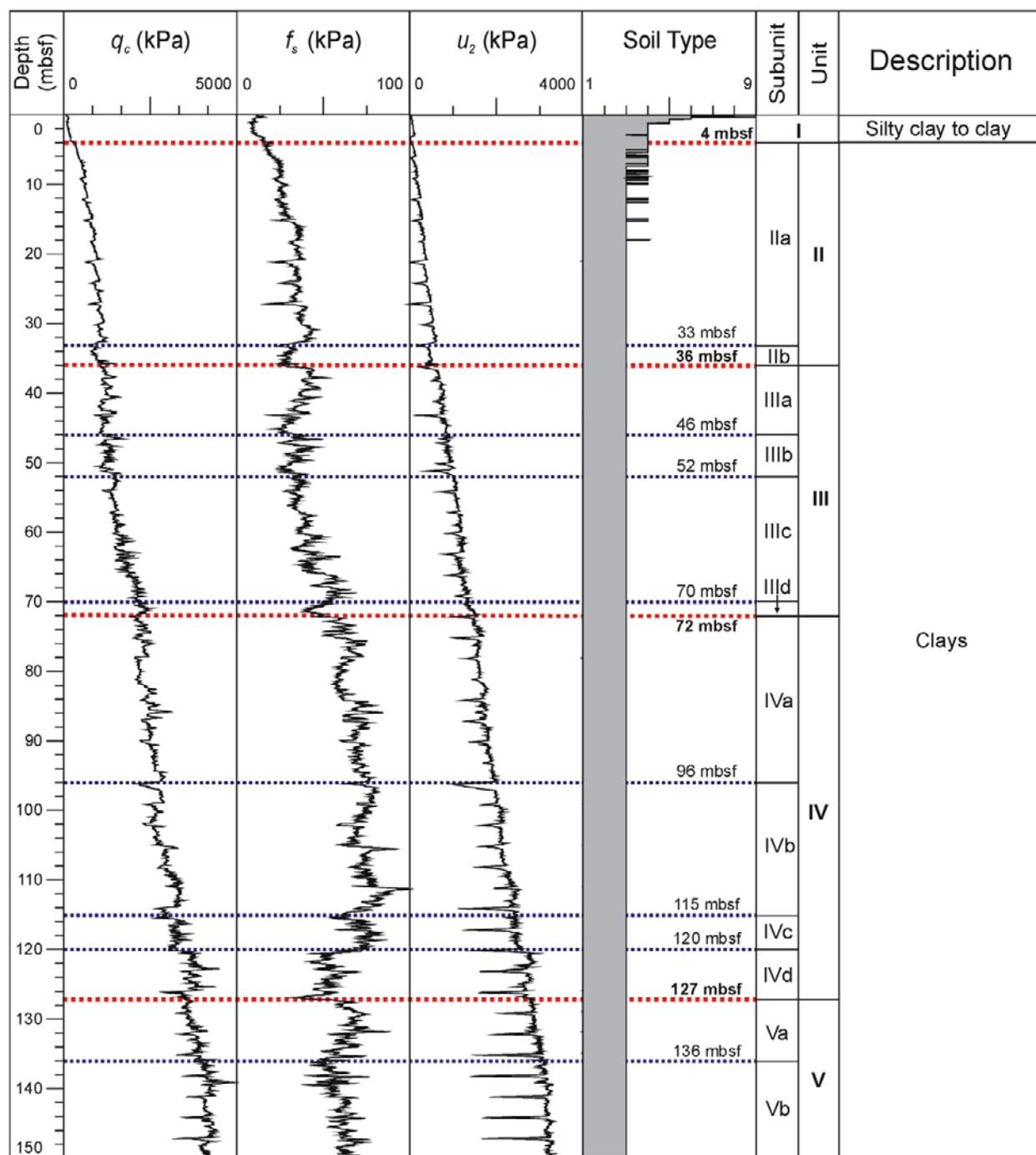
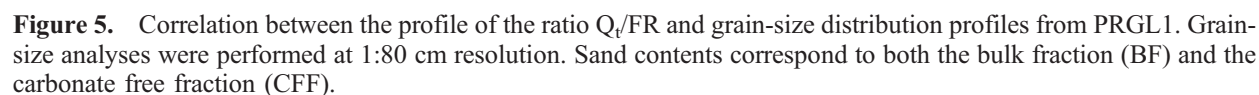


**Figure 4.** CPTU profiles from PRGL1\_3 borehole. Red dotted lines are unit boundaries that correspond to main seismic discontinuities. Blue dotted lines indicate subunit boundaries. *Robertson's* [1990] soil types based on  $Q_t/FR$  are represented at corresponding depths. Numbers in the soil type scale correspond to those in Figure 2.

classification based on  $Q_t/FR$  (Figures 4 and 7), although the one from *Ramsey* [2002] can be also considered since both classifications identify the same soil types (Figures 2 and 3).

[13] Water pressures generate significant values of cone resistance and pore pressure, which are cor-

rected to zero at seafloor. In downhole CPTU systems, the pressure conditions in the drill pipe may not be in full equilibrium with the surrounding groundwater pressure. Consequently, zero-correction can be subject to increased uncertainty that is in the order of 100 kPa [*Peuchen*, 2000]. The uncertainty for the zero-correction of the cone tip





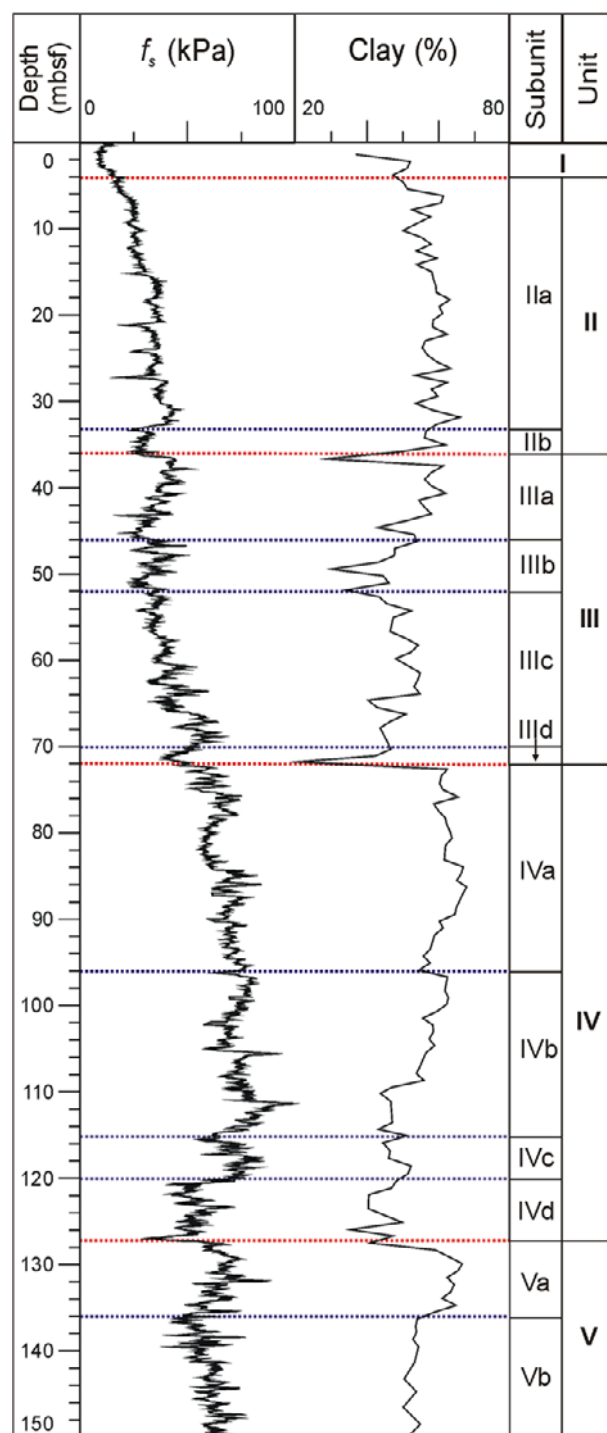


**Figure 6.** Correlation between the sleeve friction  $f_s$  profile and the clay content from PRGL1.

resistance is approximately equivalent to a factor representing the net area ratio effect, which is 0.75 for the data presented herein. The zero drift of the measured  $q_c$  and  $u_2$  is considered to be within the allowable minimum accuracy according the accuracy class selected by Fugro, following standard-

ized practice [International Society for Soil Mechanics and Geotechnical Engineering, 1999]. Therefore, we consider irrelevant the uncertainty of the derived parameters used for soil classification.

## 4.2. Stratigraphic Profiling From CPTU Profiles

[14] The transition from one layer to another is not necessarily registered as a sharp change in cone tip resistance,  $q_c$  [Lunne *et al.*, 1997]. Recent numerical analyses show that  $q_c$  in a dense sandy layer embedded in soft clays is less than its true value when the thickness of the sand layer is less than 28 cone diameters [Ahmadi and Robertson, 2005], i.e.,  $>1$  m for the cone used in our study. In contrast, for a very loose sand layer under moderate stress states (effective vertical stress  $\geq 70$  kPa) the layer should be more than eight cone diameters, i.e.,  $>0.3$  m for our study. The lower thickness of sand layers identified at PRGL2, which is 1.5 m in subunit 1c (Figure 7), is slightly above the 0.3–1 m cone accuracy.

[15] Some authors [Robertson, 1990; Lunne *et al.*, 1997] consider that the sleeve friction,  $f_s$ , is less accurate than the cone tip resistance  $q_c$  and that the pore pressure  $u_2$  measurements since  $f_s$  measures average values over the sleeve length (13 cm in our case), which tends to smooth out the record of thin layers. However, we found  $f_s$  to be the most accurate CPTU parameter for profiling the sediments at PRGL1 site, as demonstrated by its correlation with the clay content (Figure 6). The stratigraphic profile based on  $f_s$  is further supported by the  $Q_t/FR$  profile, which proves that  $f_s$  variations are, at this site, caused by changes in the cohesion that are directly related to the clay content.

## 4.3. Correlation Between CPTU-Based Geotechnical Stratigraphy and High-Resolution Seismic Reflection Profiles

[16] At site PRGL2, lithological and geotechnical subunits 1a to 1d correspond to the upper shoreface sands of the seismic unit U152 [Bassetti *et al.*, 2008, Figure 9a]. Our sandy unit 1 is bounded by a submarine erosion surface D65 atop of the geotechnical unit 2. Subunits 2a and 2b, separated by discontinuity D64, display clays with intercalations of silty clays of a lower shoreface and correspond to the seismic unit U151 [Figure 10a]. The top of the silty clayey subunit 2c, which is characterized by a slight increase in  $q_c$  and  $f_s$ , corresponds to combined discontinuity D60–D63, which separates



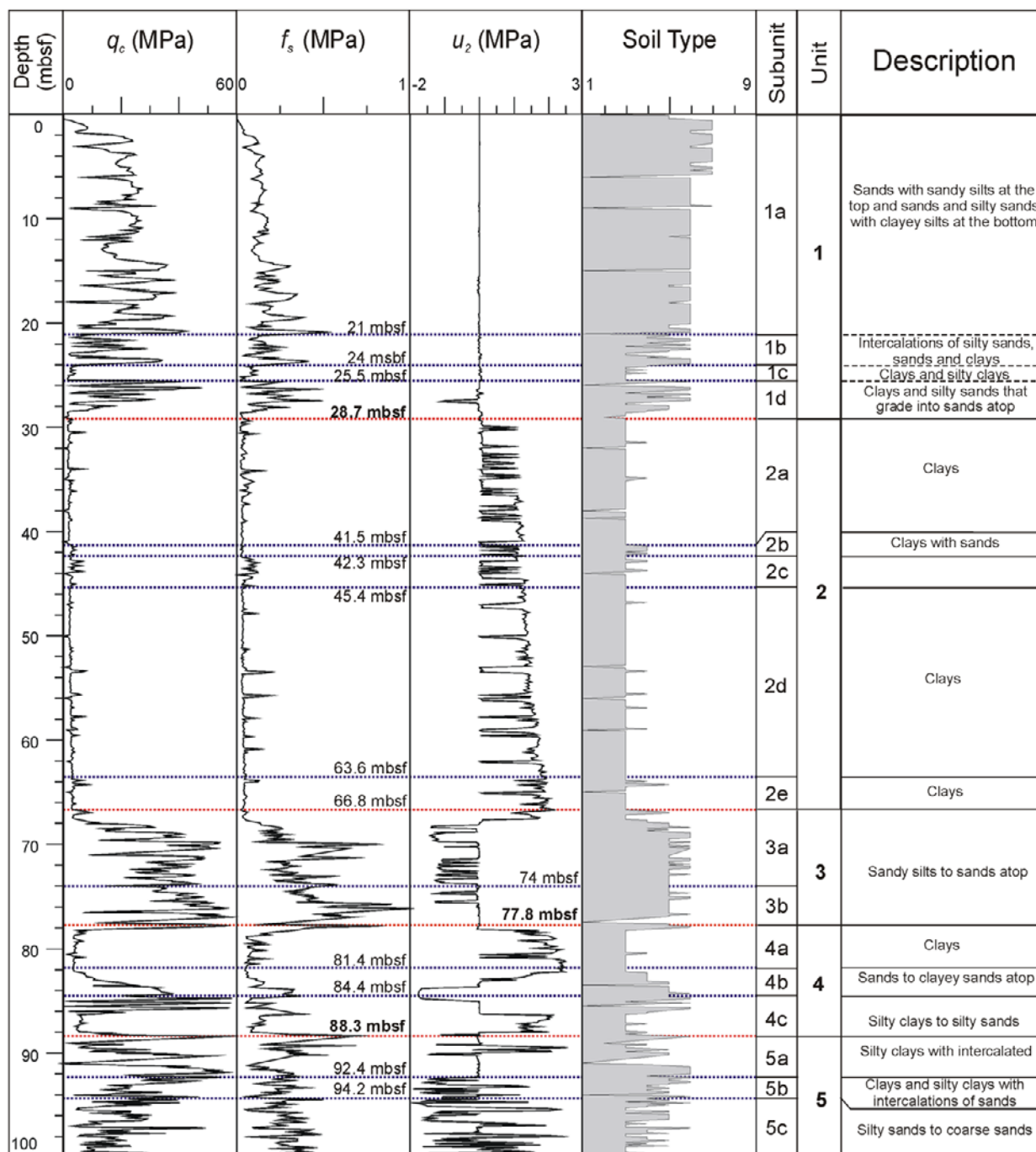


**Figure 7.** CPTU profiles from PRGL2\_1 borehole. Red dotted lines are unit boundaries that correspond to main seismic discontinuities. Blue dotted lines indicate subunit boundaries. Soil types are based on the  $Q_t/FR$  chart from Robertson [1990]. Numbers in the soil type scale correspond to those in Figure 2.

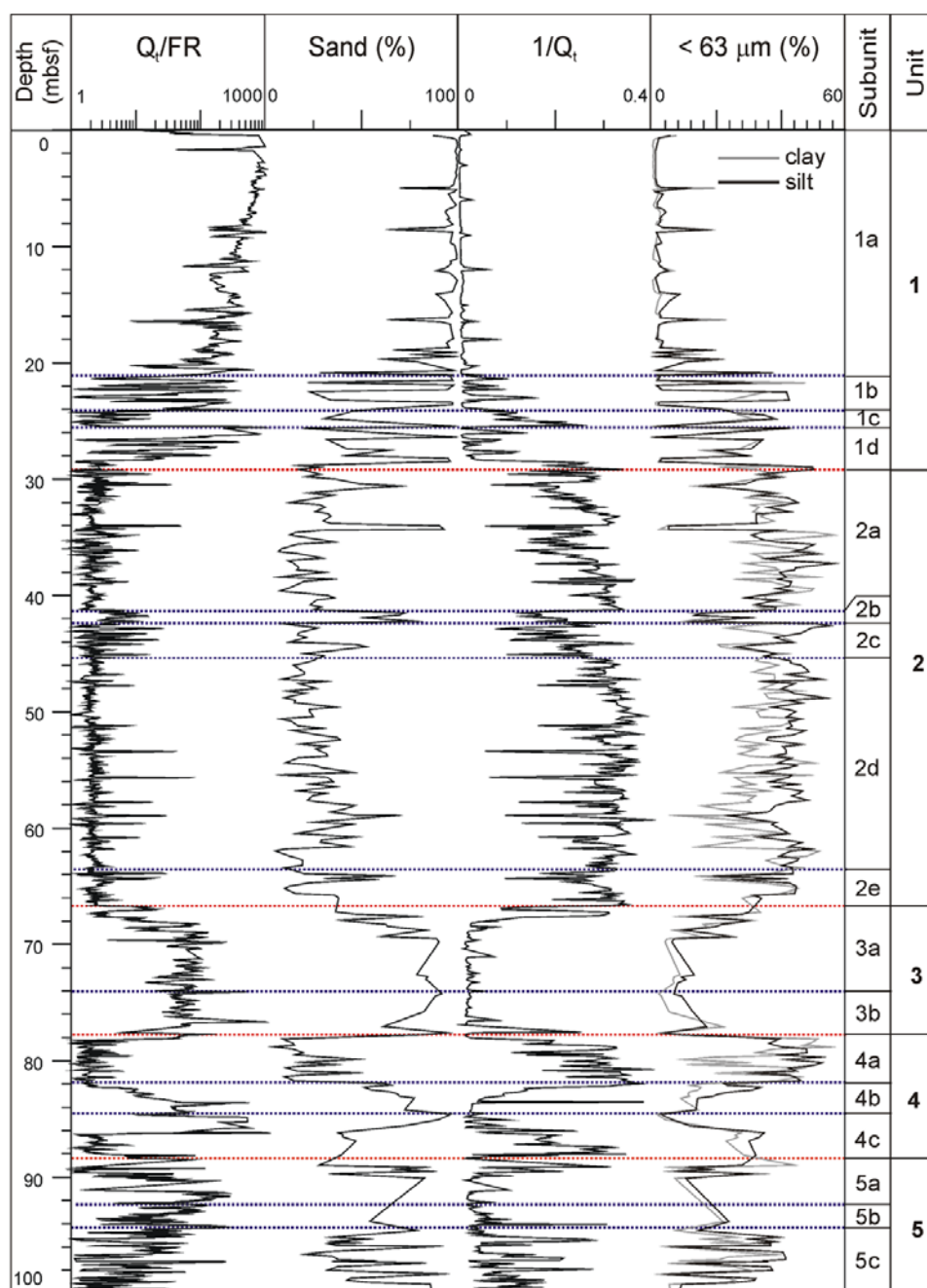


**Figure 8.** Correlation between profiles of the ratio  $Q_t/FR$  and  $1/Q_t$  and grain-size distribution profiles from PRGL2. Grain-size analyses were performed at 1:20 cm resolution in muddy sections and at 1:80 cm in cohesionless sandy sections.

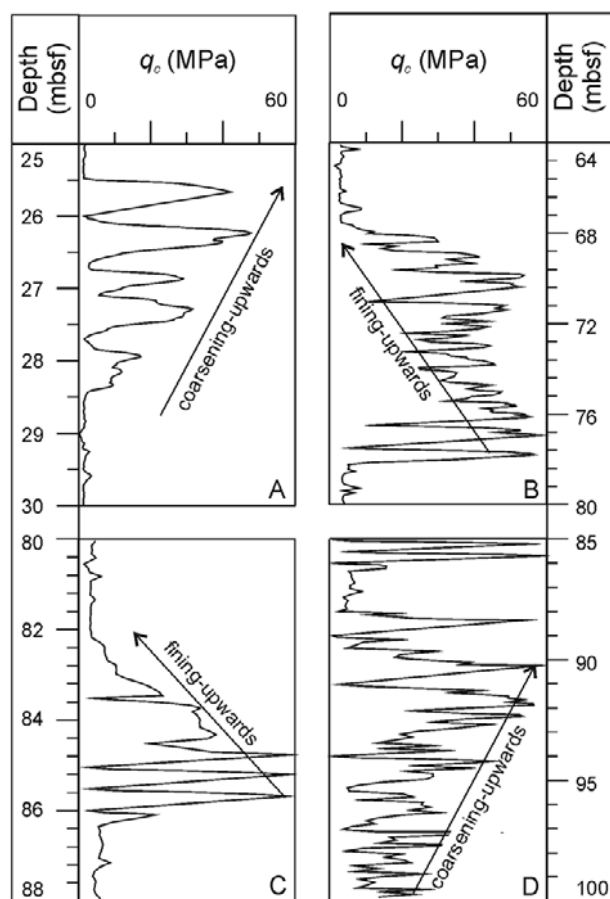


**Figure 9.** Grain-size trends at PRGL2 interpreted from cone tip resistance  $q_c$  trends. (a) Coarsening upward sequence at subunit 1d; (b) fining upward sequence at unit 7; (c) fining upward sequence at subunits 4c, 4b, and 4a; and (d) coarsening upward sequence at subunits 5c and 5b.

seismic sequence S5 (formed here by U152 and U151) from S4. D63 is an erosion surface attributed to a drop of sea level during the overall sea level fall between Marine Isotope Stage (MIS) 3 and MIS 2 [Jouet *et al.*, 2006; Bassetti *et al.*, 2008]. Clays in our subunits 2d and 2e correspond to the distal part of seismic sequence S4. The sandy unit 3 corresponds to foreshore-upper shore shoreface deposits that, in conjunction with the clayey subunit 4a, forms seismic unit S3. The underlying fining upward subunit 4b constitute seismic unit S2. The top of unit 3 corresponds to seismic discontinuity D50 and the base of subunit 4b corresponds to the combined surfaces D45-D40-D35. Nevertheless, the three coarse-grained intervals represented by positive peaks of  $q_c$  could be linked to D45-D40-D35. Although their thickness (<1 m) is slightly below the 0.3–1 m cone accuracy (Figure 10a) and it does not allow them to be

distinguished on seismic profiles, we consider these three discontinuities are closely spaced but distinct on the basis of  $q_c$  profile. Subunit 5a is separated of the coarsening upward subunits 5b and 5c by discontinuity D30, which is at the base of seismic sequence S0.

[17] At the much more lithologically homogeneous site PRGL1, we found a likely correspondence among units I to III and IV with seismic sequences S5 and S4, respectively (Figure 10b). Subunits IIb (from 33 to 36 mbsf), IIId (70–72 mbsf), and IVd (120–127 mbsf) comprise the reflectors corresponding to discontinuities D63, D60, and D50, which are found to represent intervals of variable thickness characterized by low friction measurements due to increased sand content (Figures 5 and 6). The lower unit V corresponds to S3. The rest of the boundaries between our CPTU-based subunits do correspond to specific seismic reflectors, which are seen to separate different seismic facies: subunits IIa and IIId correspond to low-amplitude hemistratified facies; IIb, IVa, IVb, Va, and Vb to facies of intermediate amplitude; and IIIa, IIIb, and IVc to facies of higher relative amplitude. Such changes in relative amplitude in the seismic record do correlate well with the CPTU-based geotechnical-stratigraphic divisions.

## 5. Conclusions

[18] The piezocone (CPTU) is a widely accepted soil classification test routinely used by geotechnical engineers. However, CPTU soil classification charts have to be used with extreme care when dealing with mixtures of marine silts and clays in similar proportions. The (undrained) behavior of these admixtures is the same as (undrained) pure clays and, consequently, they could be erroneously classified as clays. Combined normalized tip resistance  $Q_t$  and friction ratio FR profiles are very useful to identify grain-size trends in these sediment types and verify soil type classification results.

[19] The comparison of CPTU profiles with grain-size data and high-resolution seismic reflection profiles has demonstrated that among the various CPTU parameters, sleeve friction is convenient for profiling fine-grained sediments, such as those found at PRGL1 site, whereas cone tip resistance proves to be the best suited parameter in heterogeneous sequences with coarse and fine-grained sediments as at PRGL2 site. The ratio of the normalized tip resistance versus friction ratio  $Q_t/$



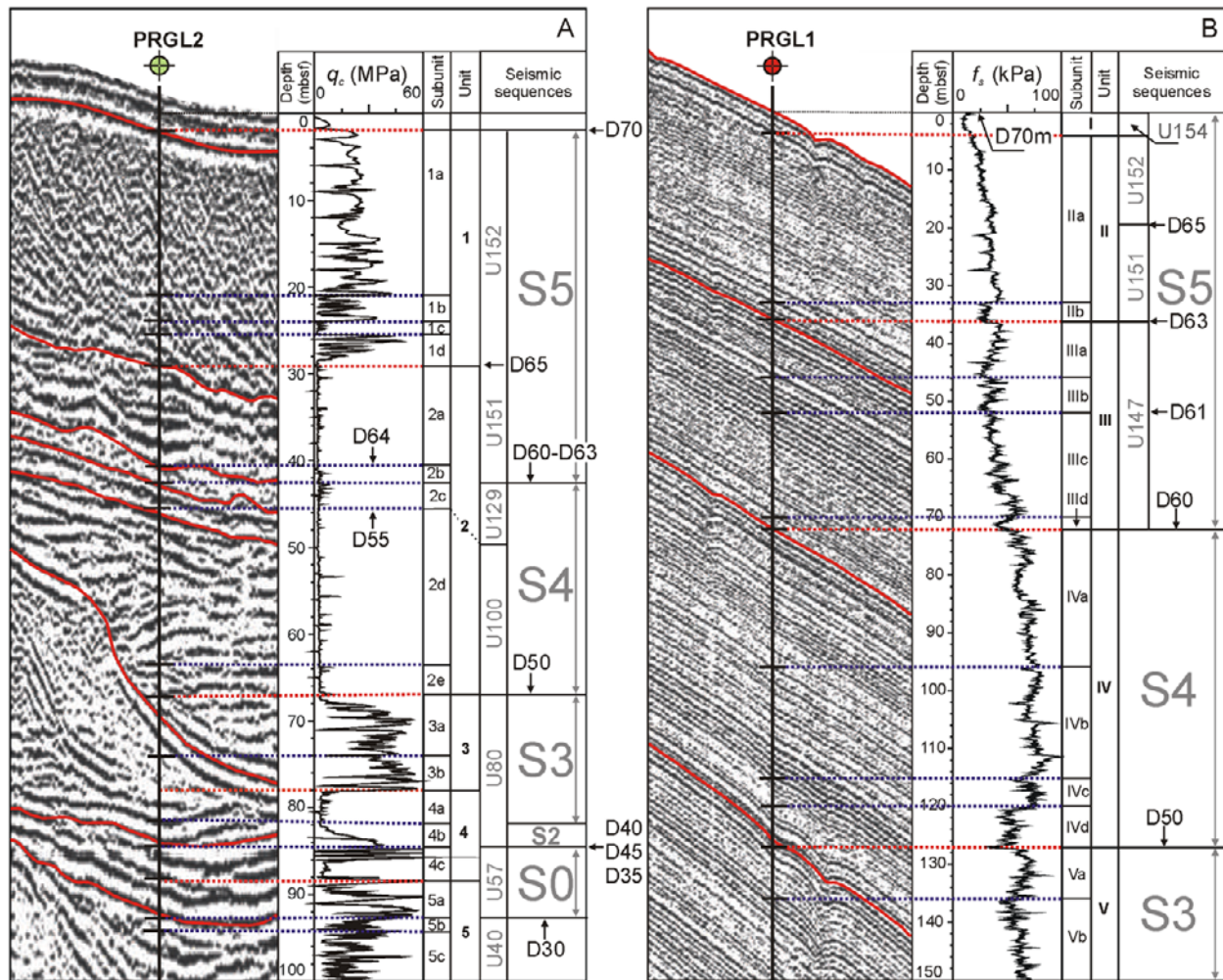


**Figure 10.** Correlation between CPTU-based geotechnical stratigraphy and seismic reflection stratigraphy at PRGL1 and PRGL2 sites. (a) CPTU-seismic reflection data correlation at site PRGL2 and (b) CPTU-seismic reflection data correlation at site PRGL1.

FR has proved to be also suitable for identifying soil stratigraphy.

[20] From the case study presented herein we conclude that in situ piezocone tests are a useful tool to interpolate and extrapolate the stratigraphic profile and the soil classification on the basis of grain size and/or seismic reflection data. The drawbacks found in the prediction of fine-grained deposits illustrate the need to further investigate soil classification methods in these sediment types.

## Notation

$q_c$  cone tip resistance, kPa.  
 $f_s$  sleeve friction, kPa.  
 $u_2$  pore pressure, kPa.

$q_t$  corrected cone resistance, equal to  $q_c + u_2(1 - a)$ , kPa.  
 $q_{net}$  net tip resistance, equal to  $q_{net} = q_t - \sigma_v$ , kPa.  
 $a$  cone area ratio (0.75 in this study).  
 $FR$  friction ratio, equal to  $f_s/q_c \cdot 100$ , %.  
 $B_q$  pore pressure ratio, equal to  $\Delta u/q_{net}$ , dimensionless.  
 $Q_t$  normalized cone resistance, equal to  $Q_t = (q_t - \sigma_v)/\sigma'_v$ , dimensionless.  
 $u_0$  in situ pore pressure, equal to  $\gamma_w \cdot z$  ( $\gamma_w$ , water unit weight;  $z$ , depth), kPa.  
 $\Delta u$  in situ excess pore pressure, equal to  $u_2 - u_0$ , kPa.  
 $\sigma_v$  total vertical stress relative to seafloor.  
 $\sigma'_v$  vertical effective stress, kPa.  
 $\phi$  particle diameter,  $\mu\text{m}$ .



## Acknowledgments

[21] The authors thank the EC PROMESS1 project (contract EVR1-CT-2002-40024). The onboard scientific party of the project has been involved in the gathering of the data and their input is very much appreciated. We thank G. Herrera (Universitat de Barcelona) for grain size analyses and E. Thereau (Ifremer) for processing the seismic data. We also acknowledge all other researchers and technicians from PROMESS1 partner institutions that have contributed in different ways to this research. Associate Editor as well as G. Verdiccio and an anonymous reviewer are thanked for their review of the manuscript. S. Lafuerza benefits from a PhD research grant by the Spanish Ministry for Education and Science. GRC Geociències Marines is funded by Generalitat de Catalunya research grants program to high quality scientific groups (ro. 2005 SGR-00152).

## References

- Ahmadi, M. M., and P. K. Robertson (2005), Thin-layer effects on the CPT qc measurements, *Can. Geotech. J.*, **42**, 1302–1317, doi:10.1139/t05-036.
- Bassetti, M. A., et al. (2008), 100-kyr and rapid sea-level changes recorded by prograding shelf sand bodies in the Gulf of Lions (Western Mediterranean Sea), *Geochem. Geophys. Geosyst.*, **9**, Q11R05, doi:10.1029/2007GC001854.
- Berné, S., M. Rabineau, J. A. Flores, and F. J. Sierro (2004a), The Impact of Quaternary global changes on strata formation, exploration of the shelf edge in the northwest Mediterranean Sea, *Oceanography*, **17**(4), 92–117.
- Berné, S., D. Carré, B. Loubrieu, J. P. Mazé, L. Morvan, A. Normand (2004b), Le Golfe du Lion, *Carte Morpho-Bathymétrique*, scale 1:250,000, IFREMER, Plouzané, France.
- Canals, M. (1985), Estructura sedimentaria y evolución morfológica del talud y el glacis continentales del Golfo de León: Fenómenos de desestabilización de la cobertura cuaternaria, Ph.D. thesis, Univ. of Barcelona, Spain.
- International Society for Soil Mechanics and Geotechnical Engineering (1999), International reference test procedure for the Cone Penetration Test (CPT) and the Cone Penetration Test with Pore Pressure (CPTU), report of the ISSMGE Technical Committee 16 on Ground Property Characterisation from in-situ testings, in *Proceedings of the Twelfth European Conference on Soil Mechanics and Geotechnical Engineering*, Amsterdam, vol. 3, edited by F. B. J. Barends et al., pp. 2195–2222, London.
- Jouet, G., S. Berné, M. Rabineau, M. A. Bassetti, P. Bernier, B. Dennielou, J. A. Flores, F. J. Sierro, and M. Taviani (2006), Shoreface migrations at the shelf edge and sea-level changes around the last glacial maximum (Gulf of Lions, NW Mediterranean), *Mar. Geol.*, **234**, 21–42, doi:10.1016/j.margeo.2006.09.012.
- Konert, M., and J. Vandenberghe (1997), Comparison of laser grain size analysis with pipette and sieve analysis: A solution for the underestimation of the clay fraction, *Sedimentology*, **44**, 523–535, doi:10.1046/j.1365-3091.1997.d01-38.x.
- Lunne, T., P. K. Robertson, and J. J. M. Powell (1997), *Cone Penetration Testing in Geotechnical Practice*, 312 pp., Blackie, New York.
- Medimap Group (2005), Morpho-bathymetry of the Mediterranean Sea, atlases and maps, scale 1:2000000, IFREMER, Plouzané, France.
- Peuchen, J. (2000), Deepwater cone penetration tests, OTC 12094, paper presented at Offshore Technology Conference, Am. Assoc. of Petrol. Geol., Houston, Tex.
- Rabineau, M., S. Berné, E. Ledrezen, G. Lericolais, T. Marsset, and M. Rotuno (1998), 3D architecture of lowstand Quaternary sand bodies on the outer shelf of the Gulf of Lions, France, *Mar. Pet. Geol.*, **15**(5), 439–452, doi:10.1016/S0264-8172(98)00015-4.
- Rabineau, M., S. Berné, D. Aslanian, J.-L. Olivet, P. Joseph, F. Guillocheau, J. F. Bourillet, E. Ledrezen, and D. Granjeon (2005), Sedimentary sequences in the Gulf of Lion: A record of 100,000 years climatic cycles, *Mar. Pet. Geol.*, **22**, 775–804, doi:10.1016/j.marpetgeo.2005.03.010.
- Ramsey, N. (2002), A calibrated model for the interpretation of cone penetration tests (CPTs) in North Sea Quaternary soils, paper presented at the Offshore Site Investigation and Geotechnics: Diversity and Sustainability, Soc. for Underwater Technol., London.
- Robertson, P. K. (1990), Soil classification using the cone penetration test, *Can. Geotech. J.*, **27**, 151–158, doi:10.1139/t90-014.